

PAPER

[View Article Online](#)
[View Journal](#) | [View Issue](#)Cite this: *Dalton Trans.*, 2021, **50**,
3178Calcium catalyzed enantioselective intramolecular
alkene hydroamination with chiral C₂-symmetric
bis-amide ligands†Philipp C. Stegner, Jonathan Eyselein, Gerd M. Ballmann, Jens Langer, 
Jochen Schmidt and Sjoerd Harder *

The chiral building block (*R*)-(+)-2,2'-diamino-1,1'-binaphthyl, (*R*)-BINAM, which is often used as backbone in privileged enantioselective catalysts, was converted to a series of *N*-substituted proligands **R1**-H₂ (R = CH₂tBu, C(H)Ph₂, PPh₂, dibenzosuberane, 8-quinoline). After double deprotonation with strong Mg or Ca bases, a series of alkaline earth (Ae) metal catalysts **R1**-Ae·(THF)_n was obtained. Crystal structures of these C₂-symmetric catalysts have been analyzed by quadrant models which show that the ligands with C(H)Ph₂, dibenzosuberane and 8-quinoline substituents should give the best steric discrimination for the enantioselective intramolecular alkene hydroamination (IAH) of the aminoalkenes H₂C=CHCH₂CR'₂CH₂NH₂ (CR'₂ = CPh₂, CCy or CMe₂). The dianionic **R1**²⁻ ligand in **R1**-Ae·(THF)_n functions as reagent that deprotonates the aminoalkene substrate, while the monoanionic (**R1**-H)⁻ ligand formed in this reaction functions as a chiral spectator ligand that controls the enantioselectivity of the ring closure reaction. Depending on the substituent R in the BINAM ligand, full cyclization of aminoalkenes to chiral pyrrolidine products as fast as 5 minutes was observed. Product analysis furnished enantioselectivities up to 57% ee, which marks the highest enantioselectivity reported for Ca catalyzed IAH. Higher selectivities are impeded by double protonation of the **R1**²⁻ ligand leading to complete loss of chiral information in the catalytically active species.

Received 18th January 2021,
Accepted 1st February 2021

DOI: 10.1039/d1dt00173f

rsc.li/dalton

Introduction

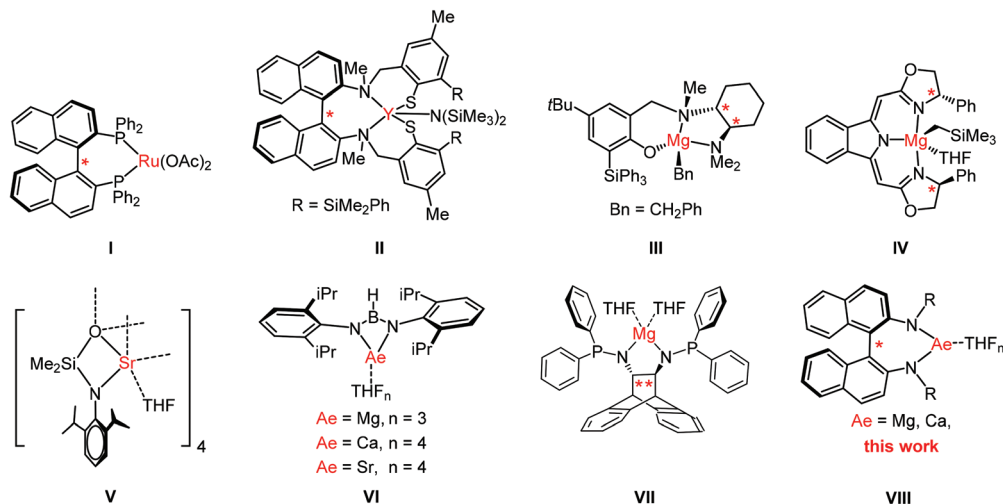
The binaphthalene scaffold is a classic textbook example for axial chirality that received great attention in the field of asymmetric catalysis.¹ As the chiral building block of a variety of highly competent catalysts, the binaphthalene motive earned the title “privileged structure”.² Its phosphorous derivative BINAP (*e.g.* in **I**) has written history as chiral backbone for Noyori's Nobel prize winning catalysts.³ It comes as no surprise, that the *N,N*- or *N,O*-chelating analogues BINAM and NOBIN, respectively, have been used as chiral building blocks in catalysts of metals that need harder ligands, like the lanthanides. For example, catalyst **II** was found to be highly effective in asymmetric intramolecular alkene hydroamination (IAH).⁴ Besides various application in catalysis, rare earth elements are of great importance in key technologies like petroleum refining, permanent magnets or superconductors. This results

in high prices, limited supply and a high, steadily growing demand.⁵ Alkaline earth (Ae) metals are an attractive alternative to lanthanide metals. Like the lanthanides, their bonding and reactivity is mainly influenced by electrostatics and size. In contrast to the lanthanides, the benign Ae metals Mg and Ca are highly abundant and low-cost.

While homogeneous catalysis with group 2 metals has come a long way,^{6,7} enantioselective catalysis with Ae metal catalysts was found to be a major challenge. Although there are various examples of enantioselective 1,4-additions or [3 + 2] cycloaddition reactions that are mainly catalyzed by the Lewis acidic Ae metal,⁸ there are hardly examples of efficient chiral Ae metal catalysts in which high ligand basicity is essential. Most efforts concentrated on IAH catalysis,^{6a,9–18} an application which since the start of group 2 metal catalysis has been intensively investigated.^{7,19,20} Hultsch and coworkers reported a chiral Mg catalyst (**III**) for IAH that gave very high enantioselectivities (>90% ee).¹² Also for enantioselective ketone hydroboration some highly efficient chiral catalysts have been reported. The Gade group developed chiral catalyst **IV**^{21a} while Rüping and coworkers reported a less defined catalyst system based on Mg η Bu₂, LiCl and chiral BINOL derivatives.^{21b}

Inorganic and Organometallic Chemistry, Friedrich-Alexander-Universität Erlangen-Nürnberg, Egerlandstraße 1, 91058 Erlangen, Germany

† Electronic supplementary information (ESI) available. CCDC 2056448–2056453. For ESI and crystallographic data in CIF or other electronic format see DOI: 10.1039/d1dt00173f



The scope of catalytic reactions and substrates could be enormously expanded, if one would be able to extend this research to more reactive catalysts based on the heavier Ae metals Ca, Sr or Ba. Most attempts to control the enantioselectivity in Ca catalyzed reactions failed so far.^{10,12–15} There are two major reasons for this shortcoming. Group 2 metal complexes exhibit highly ionic bonds and therefore have highly fluxional coordination geometries instead of the rigid chiral structures needed for efficient stereocontrol. Apart from that, high dynamics also affects the stability of heteroleptic catalysts. The prototypical enantioselective catalyst L^*-Ae-R consists of a chiral spectator ligand L^* , that is needed to exhibit enantiocontrol, and a reactive group R for substrate deprotonation. The Schlenk equilibrium (Scheme 1a) leads to the detrimental formation of the achiral reactive species AeR_2 , resulting in loss of stereocontrol. The dynamics and challenge to control the Schlenk equilibrium both strongly increase with Ae metal size ($Mg > Ca > Sr > Ba$).²² Since the reactivity and activity of Ae metal catalysts generally also increases down group 2, these conflicting trends impede the development of enantioselective, more reactive, heavier Ae metal catalysts.

We recently developed a series of catalysts with non-innocent N,O - or N,N -chelating ligands (V–VI).²³ The bidentate ligands in these complexes function at the same time as spectator and reactive ligand. The advantage of these systems with cooperative bidentate ligands is that Schlenk equilibria do not play a role. Metal exchange would lead to larger aggregates or

oligomeric structures that are entropically disadvantaged (Scheme 1b). We recently reported on a Mg catalyst (VII) with a chiral N,N -chelating ligand that cooperatively acts as chiral spectator and deprotonation agent in IAH but only very low enantioselectivities of <10% ee were achieved.¹² Herein, we report the extension of this approach towards privileged, axially chiral, non-innocent BINAM ligands (VIII) and their application as enantiopure proton shuttles in IAH.

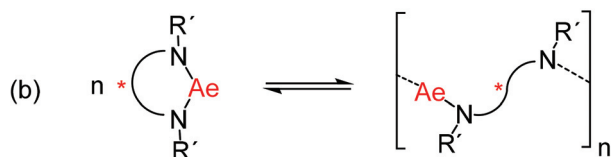
Results and discussion

Catalyst syntheses and characterization

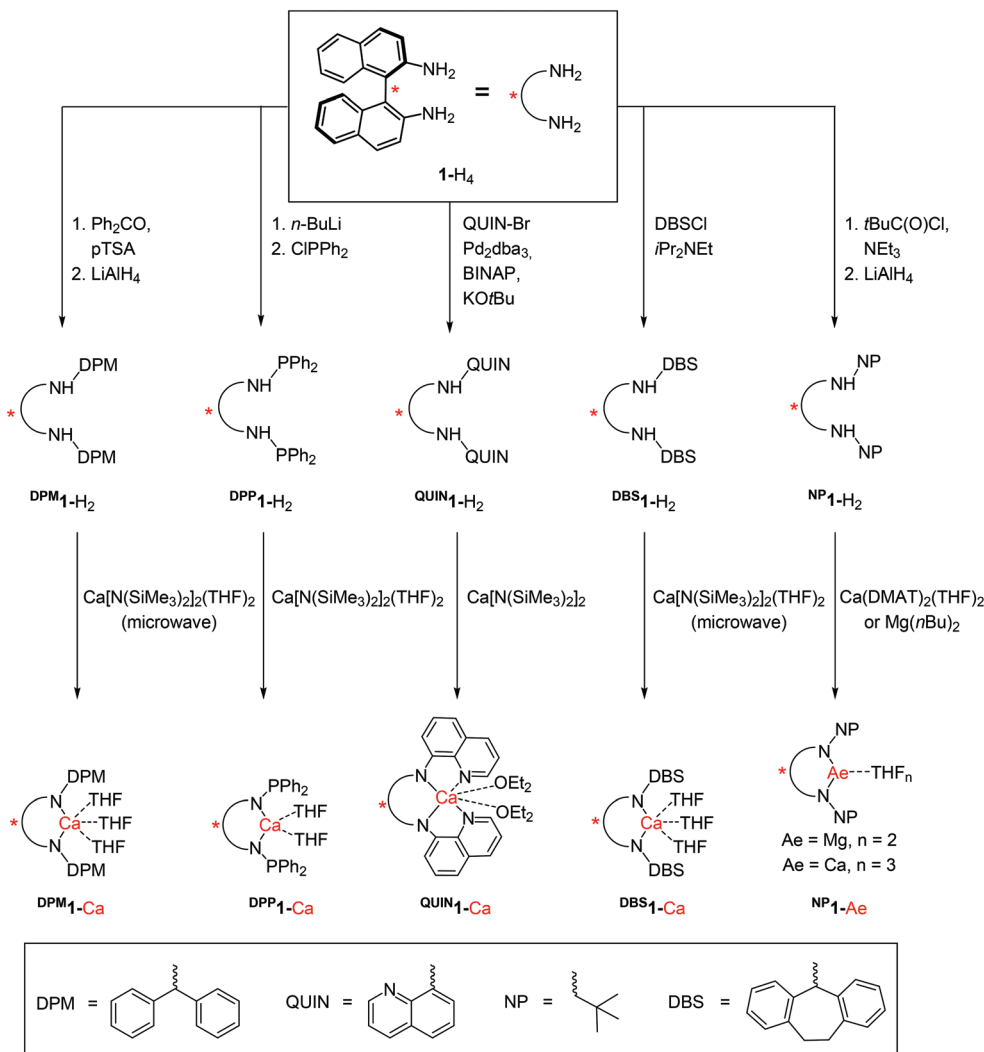
Racemic BINAM was synthesized by reacting hydrazine and 2-naphthol, following the protocol of Clemons and Dawson.²⁴ The purification process was modified, using solvent extraction and subsequent recrystallization. This improvement avoids the elaborate precipitation of the corresponding ammonium salt and the use of larger quantities of diethyl-ether. Subsequent resolution according to a literature protocol furnished optically pure (*R*)-BINAM (**1-H₄**, ee >99%) on a multi-gram scale.²⁵

Starting from (*R*)-BINAM, a selection of C_2 -symmetric N,N -bidentate ligands (**R1-H₂**), with varying steric and electronic properties was synthesized (Scheme 2). **DPM1-H₂** was prepared by condensation with benzophenone and subsequent reduction with $LiAlH_4$. Further ligands were prepared according to literature procedures.^{26–29} All ligands were obtained as crystalline solids in moderate to good yields between 60% and 85%. Purification was achieved by column chromatography and the purity was confirmed by NMR spectroscopy and elemental analysis.

Deprotonation of the (*R*)-BINAM ligands **R1-H₂** gave rise to a series of fully characterized enantiopure, axial chiral Ae organometallics (Scheme 2). All complexes were found to be pure according to elemental analysis and were obtained as crystalline solids. Ligand deprotonation with MgH_2 , $Ca[N(SiMe_3)_2]_2(THF)_n$ ($n = 0$ or 2) or $Ca(DMAT)_2(THF)_2$ gave the corresponding Mg and Ca complexes in good to excellent yields ranging from 70% to 94%. Acidic ligands like **DPP1-H₂**



Scheme 1 (a) Ligand exchange results in a Schlenk equilibrium. (b) Ligand exchange results in oligomeric species. L^* = chiral spectator ligand; R = reactive group; R' = bulky residue.



Scheme 2 Synthesis of various (*R*)-BINAM derived ligands $\text{R}^1\text{-H}_2$ and complexes $\text{R}^1\text{-Ae}$.

and $\text{QUIN}^1\text{-H}_2$ were smoothly deprotonated by the weak base $\text{Ca}[\text{N}(\text{SiMe}_3)_2]_2(\text{THF})_2$ at room temperature, while for the less acidic ligands $\text{DPM}^1\text{-H}_2$ and $\text{DBS}^1\text{-H}_2$ microwave irradiation was needed. To examine the influence of the Ae center on the catalytic performance, $\text{NP}^1\text{-Mg}$ and $\text{NP}^1\text{-Ca}$ were prepared.

Deprotonation of this alkylated bis-amine with $\text{Ae}[\text{N}(\text{SiMe}_3)_2]_2(\text{THF})_2$ ($\text{Ae} = \text{Mg}, \text{Ca}$) failed due to insufficient basicity of the metal reagent ($\text{p}K_a(\text{Me}_3\text{Si})_2\text{NH} = 25.8$),³⁰ however, the stronger bases $\text{Mg}(n\text{Bu})_2$ and $\text{Ca}(\text{DMAT})_2(\text{THF})_2$ reacted smoothly. ^1H and ^{13}C NMR spectroscopy in aromatic solvents revealed the retention of C_2 -symmetry in solution. Heating toluene solutions of the $\text{R}^1\text{-Ae}$ complexes to 100 °C showed even after several days no signs of decomposition or ligand redistribution, which would lead in this case to higher aggregates or polymeric structures (Scheme 1b). Also the enantiopurity of the ligands was preserved. This proves their robustness at higher temperatures, which is a vital prerequisite for successful application in asymmetric catalysis. All compounds crystallize as C_2 -symmetric monomers, with 1–3 ether ligands

(Et_2O or THF) and their crystal structures were determined by single crystal X-ray diffraction. A comparison of their structures led to following conclusions:

(1) Metal coordination numbers vary from 4 ($\text{NP}^1\text{-Mg}$, $\text{DPP}^1\text{-Ca}$), 5 ($\text{DBS}^1\text{-Ca}$, $\text{DPM}^1\text{-Ca}$, $\text{NP}^1\text{-Ca}$) to 6 ($\text{QUIN}^1\text{-Ca}$). The Ca complexes show increasing Ca–O(THF) bond lengths with increasing metal coordination number. Discussion of the Ca–N bond lengths is complicated by the various *N*-substituents.

(2) The Ca–N bond lengths are also influenced by the Lewis basicity of the N donor. The latter depends on the nature of the substituent which can either stabilize or destabilize the negative charge. This becomes apparent by comparing the Ca–N distances in $\text{DPM}^1\text{-Ca}$ (2.299(2) Å) with those in the less basic PPh_2 derivative $\text{DPP}^1\text{-Ca}$ (2.320(2) Å). Simultaneously, the P–N distance is shortened from 1.704(2) Å for $\text{DPP}^1\text{-H}_2$ to 1.682(2) Å for $\text{DPP}^1\text{-Ca}$ upon deprotonation, indicating partial charge delocalization from the electron density on N to the PPh_2 moiety.³¹ Similar stabilization of negative charge by an $\alpha\text{-PPh}_2$ substituent was observed in **VII**.¹²

(3) For the **NP1**-ligand, both the Mg and Ca complexes could be structurally characterized. The Ca–N and Ca–O bonds are 0.333 Å and 0.364 Å longer than the corresponding Mg–N and Mg–O bonds, which is more than would be expected based on the 0.28 Å difference in ionic radii (6-coordinate: Mg 0.72 Å, Ca 1.00 Å).³² This is due to the difference in coordination numbers (4 vs. 5). Difference in metal size also causes considerable differences in the (N)C–C–C–C(N) torsion angles. While the naphthyl groups in **NP1**–Mg are close to perpendicular to each other (90.9(3)°) a considerably larger torsion angle of 115.4(7)° is needed to accommodate the larger Ca metal.

(4) Deprotonation of **R1**–H₂ and *N,N*-chelation of the Ae metal in general widens the torsion angle between the naphthyl planes. The (N)C–C–C–C(N) torsion angle of 86.7(3)° measured for **DPP1**–H₂,¹⁷ expands to 107.1(3)° upon forming the Ca complex **DPP1**–Ca. The torsion angles in the Ca complexes range from 107.1(3)° to 115.4(7)°, which means a slight increase in comparison to the parent molecule BINAM (**1**–H₄) is 106.6(2)°.³³ The only exception is found for **QUIN1**–Ca which displays a reduced torsion angle of 78.9(4)° in order to enable coordination of the quinoline moieties.

Fig. 1 shows quadrant diagrams of the crystal structures of all catalysts in which the ether ligands have been removed for clarity (Table 1). The catalysts are viewed along their C₂-symmetry axis and the horizontal dividing line is congruent with the N–Ae–

N plane. The environment around the metal is divided equally into 4 quadrants. These models give a good estimation of steric biasing and may be useful in prediction of the catalyst's performance in terms of enantioselectivity control. The diagrams predict that the **DPM1**-, **DBS1**- and **QUIN1**-ligands are favorable.

Catalysis

The catalytic potential of all catalysts in the cyclization of unactivated amino-alkene substrates (H₂C=CHCH₂CR'₂CH₂NH₂ = **R'2**) to the corresponding optically active heterocycles (**R'6**) has been investigated. Clean conversion, without formation of additional side-products is observed. The exclusive formation of pyrrolidines implies that double bond functionalization proceeds in Markovnikov fashion which is expected for IAH with Ae metal catalysts.^{7,9–18}

Ethereal solvents have a detrimental effect on the catalytic activity due to competition with substrate coordination. Therefore, all reactions have been carried out in aromatic solvents. Conversion is accomplished with increasing difficulty along the sequence: Ph-2 < Cy-2 ≪ Me-2. This tendency is explained by the Thorpe–Ingold-effect: larger R' substituents favor and accelerate the intramolecular ring closure.³⁴

In all cases the Ca catalyst **NP1**–Ca was found to be considerably more active than its Mg analogue **NP1**–Mg (Table 2, entries: 3 vs. 4; 9 vs. 10; 15 vs. 16). *E.g.* **NP1**–Ca is about 9 times

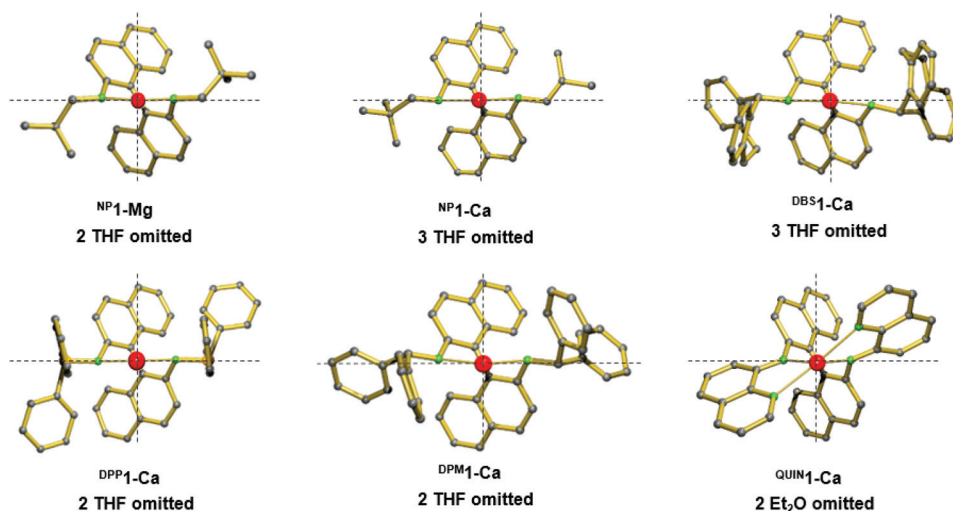
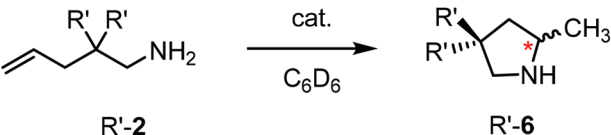
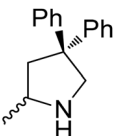
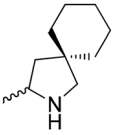
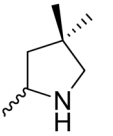


Fig. 1 Quadrant diagrams for chiral C₂-symmetric Mg and Ca catalysts. All hydrogen atoms and coordinated solvents are omitted for clarity. Metals in red and nitrogen atoms in green.

Table 1 Selected bond distances (Å) and angles (°) for chiral alkaline earth metal complexes; when possible bond values are given as average value

Compound	Average Ae–N	Average Ae–O	N–Ae–N	Torsion Angle (N)C–C–C–C(N)
DPP1 –Ca	2.320(2)	2.299(2)	118.0(7)	107.1(3)
Quin1 –Ca	2.355(3)	2.412(3)	85.2(9)	78.9(4)
NP1 –Mg	1.989(3)	2.022(2)	118.0(1)	90.9(3)
NP1 –Ca	2.322(7)	2.386(4)	120.6(2)	115.4(7)
DBS1 –Ca	2.379(2)	2.401(2)	118.2(8)	112.9(3)
DPM1 –Ca	2.299(2)	2.324(2)	117.6(7)	112.5(3)

Table 2 Catalytic IAH with various enantiopure C₂-symmetric (R)-BINAM Mg or Ca catalysts

							
Entry	Product	Catalyst	Loading [mol%]	T [°C]	T	Conv. [%]	ee [%]
1		DBS-1-Ca	10	RT	3 d	99	57
2		DPM-1-Ca	10	RT	1 d	99	32
3		NP-1-Ca	5	RT	5 min	99	18
4		NP-1-Mg	5	RT	45 min	99	13
5		DPP-1-Ca	10	100 °C	1 d	94	4
7		DBS-1-Ca	10	60 °C	20 h	99	27
8		DPM-1-Ca	10	60 °C	3 h	99	16
9		NP-1-Ca	5	RT	10 min	99	13
10		NP-1-Mg	5	60 °C	3 h	99	7
11		DPP-1-Ca	10	100 °C	3 d	—	—
13		DBS-1-Ca	10	100 °C	20 h	99	27
14		DPM-1-Ca	10	100 °C	1 d	99	14
15		NP-1-Ca	5	60 °C	1 h	99	10
16		NP-1-Mg	10	100 °C	3 d	—	—
18		DPP-1-Ca	10	100 °C	3 d	—	—

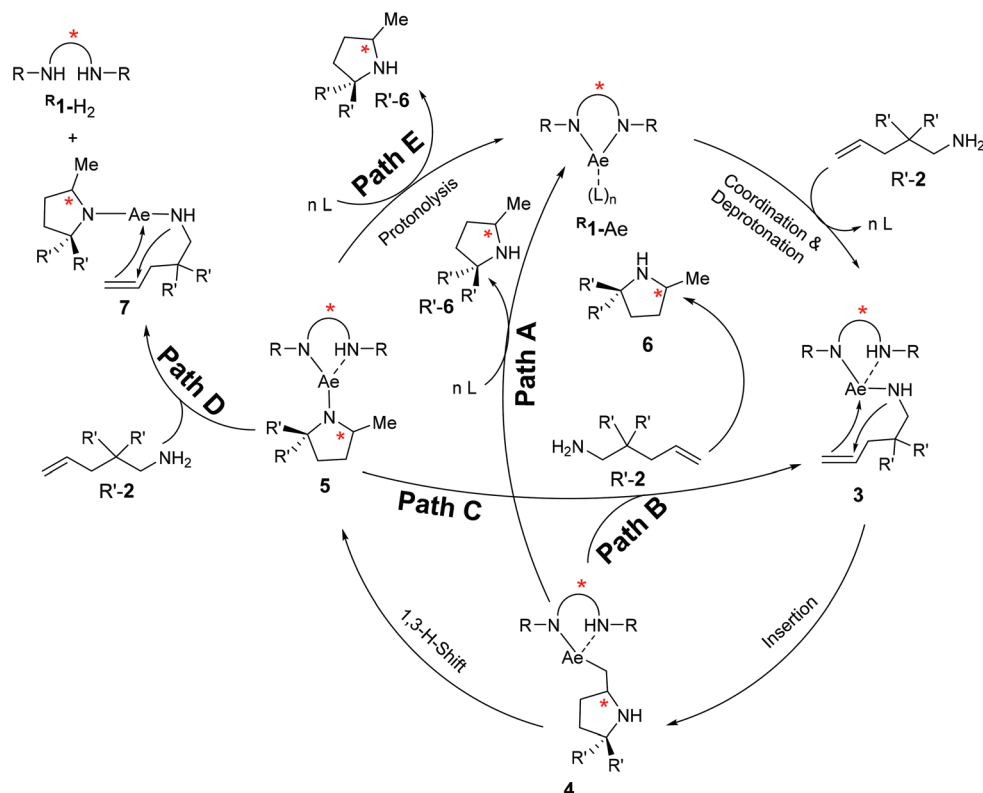
faster in the cyclization of Ph-2 than **NP**1-Mg. Conversion of Cy-2 requires heating for **NP**1-Mg and the most challenging substrate Me-2 remains inert towards cyclization with **NP**1-Mg even after several days at 100 °C. In contrast smooth cyclization of both substrates is catalyzed by **NP**1-Ca. Similar reactivity differences between Mg and Ca catalysts have been reported for **VI**.^{23b,35} Direct comparison between **VI** and **NP**1-Ca shows that the BINAM catalysts are considerably more active, even with only half the catalyst loading. Due to its superior activity, further research was exclusively conducted on Ca catalysts.

The Ca catalysts are increasingly more active along the row: **DPP**1-Ca < **DBS**1-Ca < **DPM**1-Ca < **NP**1-Ca, showing that the substituent on N has a decisive influence. Catalyst activities are determined by the steric bulk of the substituent. **NP**1-Ca bears small substituents, which results in an open coordination sphere and full conversion of Ph-2 within 5 min. In contrast **DBS**1-Ca bears large residues, shielding the catalytically active Ca center, requiring 3 days for cyclization, despite using twice the amount of catalyst. In addition, the basicity of the chiral ligand, which in this concept also acts as the base for substrate deprotonation, has an influence on conversion rates. Although the catalysts **DPP**1-Ca and **DPM**1-Ca are sterically very similar, the catalyst with the more Brønsted basic ligand (**DPM**1-Ca) yields faster substrate deprotonation and subsequent ring closure than **DPP**1-Ca in which the amide groups are stabilized by α-PPh₂ substituents. Full conversion of Cy-2 with **DPM**1-Ca takes 3 h at 60 °C, while the structurally similar, but less basic catalyst **DPP**1-Ca gave no conversion, despite heating to 100 °C for 3 days. The most active catalyst **NP**1-Ca, carrying small but electron-releasing neopentyl substituents at N, combines these steric and electronic advantages.

After cyclization, chiral pyrrolidine products (**R'**-6) were obtained. The enantioselectivity of IAH was determined by converting these pyrrolidines to diastereomers by derivatization with *O*-acetyl mandelic acid or Mosher's chloride and subsequent NMR analysis. Enantiomeric excess (ee) was determined by integration of the signals for the two different diastereomers using ¹H or ¹⁹F NMR spectroscopy.

Comparing the enantiocontrol for the five different catalysts shows that the worst stereoselectivities are obtained for catalysts with neopentyl-substituted ligands, **NP**1-Mg and **NP**1-Ca, and the catalyst with PPh₂ substituents, **DPP**1-Ca. The low enantioselectivity for the latter catalyst may be explained by its low activity and the inherently harsh reaction conditions needed for conversion. In addition, also the quadrant diagram for **DPP**1-Ca (Fig. 1) does not show perfect steric discrimination. Although quadrant discrimination for **NP**1-Ca seems more advantageous, the neopentyl substituents are small and clearly turned backwards, only exerting limited steric pressure on the metal coordination sphere. Catalysts **NP**1-Mg and **NP**1-Ca gave both very poor stereocontrol but, contrary to published trends,^{6a,9} the Ca catalyst consistently gave slightly better selectivities. The highest enantioselectivities have been obtained for catalyst **DBS**1-Ca in which a very bulky and rigid dibenzosuberane (DBS) substituent leads to efficient quadrant discrimination and steric pressure.

Using this catalyst, the substrate with the bulkiest substituents (Ph-2) gave the highest enantioselectivity of 57% ee. To the best of our knowledge this is the highest ee value published for a Ca based IAH catalyst.⁶ Attempts to further increase the selectivity of **DBS**1-Ca using lower temperatures, were hampered by a drastic increase in reaction times (25%



Scheme 3 Proposed catalytic cycle for the intramolecular alkene hydroamination with R^1 -Ae catalysts.

conversion within 7 days at 10 °C). We propose a mechanism that is based on previously reported catalytic cycles for catalysts **V**, and **VI** (Scheme 3).^{12,23b}

The bidentate BINAM ligand in R^1 -Ae acts as a non-innocent ligand, actively participating as a chiral proton shuttle. In the first step the BINAM ligand functions as deprotonating agent. In the second rate-determining ring closure step, the protonated BINAM- H^+ acts as a chiral spectator ligand determining the enantioselectivity. This results in highly reactive alkyl-Ae intermediate **4** which either is subject to immediate protonolysis (Path A and B) or converts to the more stable amide **5**, which is subsequently protonated (Path C and E). There are different alternatives for the protonation step, proceeding either in an intramolecular (Path A and E) or in an intermolecular (Path B and C) fashion. Additionally, it has also been proposed that ring closure and protonation may proceed in one concerted step *via* a transition state that involves the presence of a second aminoalkene.³⁶

During monitoring of the catalytic reaction with 1H NMR, it was noted that the concentration of fully protonated ligand (R^1 - H_2) steadily increased to *circa* 10%. Since all glassware was flame dried and solvents and substrates were thoroughly dried, hydrolysis by traces of moisture seems unlikely. It is therefore proposed that, starting from intermediate **5**, the second ligand protonation proceeds by reaction with the aminoalkene substrate (Path D). Elimination of the R^1 - H_2 ligand would result in complete loss of chiral information and this

might be the origin of the poor enantioselectivity. Since the concentration of R^1 - H_2 is steadily raised during conversion, the enantioselectivity should decrease with conversion. Indeed, quenching the IAH reaction of Ph-2 with catalyst **DBS** 1 -Ca after 40% conversion gave a higher enantioselectivity of 65% ee. This observation substantiates ligand loss *via* double protonation as the main degradation process of this catalytic system.

Reasoning that this degradation process becomes less likely by providing enhanced metal chelation, the catalyst **QUIN** 1 -Ca was introduced. Indeed, additional metal chelation by the 8-quinolinyl substituent gave a more rigid, well-defined, structure with good quadrant discrimination. Reactions with aminoalkene substrates did not lead to formation of **QUIN** 1 - H_2 which proves that it is less sensitive to complete loss of the chiral ligand. However, the additional quinoline arms also block the metal coordination sites and renders the complex fully inert in IAH catalysis. Even the addition of the strong, non-nucleophilic, organic phosphazene base P4-*t*Bu did not lead to catalytic activity. This methodology, in which a neutral organic strong base and a Lewis acidic metal salt cooperatively form a catalyst for ring closure of aminoalkenes, has been recently introduced.¹⁷ The complete inactivity of the **QUIN** 1 -Ca/P4-*t*Bu acid/base combination indicates that **QUIN** 1 -Ca is insufficiently Lewis acidic to engage in hybrid catalysis. Further future research is directed to obtain a balanced ratio between catalyst stability and reactivity.

Conclusion

A series of novel chiral Ae catalysts (R^1 -Ae), based on the axially chiral ligand (*R*)-BINAM, were synthesized in good to excellent yields. All compounds were fully characterized using NMR spectroscopy, elemental analysis and X-ray diffraction. Facile ligand exchange reactions by the Schlenk equilibrium were not observed, even not when heated to 100 °C for several days. Full conversion in catalytic IAH of unactivated aminoalkenes was achieved at room temperature as fast as 5 minutes. Enantioselectivities up to 57% ee have been determined, which to the best of our knowledge marks the highest enantioselectivity in Ca catalyzed IAH. Double protonation of the dianionic BINAM ligand during catalysis was identified as the main catalyst degradation process. Improving catalyst stability by enhanced chelation resulted in complete catalyst inactivity. Although progress was achieved, these investigations clearly demonstrate that enantioselective IAH catalysis with more reactive heavier Ae metal catalysts remains a challenge.

Conflicts of interest

There are no conflicts to declare.

Acknowledgements

We thank Antigone Roth for elemental analysis and SH thanks the Deutsche Forschungsgemeinschaft for funding of this project (HA 3218/8-1).

References

- (a) K. H. Hellwich, *Stereochemie—Grundbegriffe*, Springer, Berlin, Heidelberg, 2019; (b) S. G. Telfer and R. Kuroda, *Coord. Chem. Rev.*, 2003, **242**, 33.
- (a) T. P. Yoon and E. N. Jacobsen, *Science*, 2003, **299**, 1691; (b) J. Wang, L. Hao, Y. Xinhong and W. Wang, *Org. Lett.*, 2005, **7**, 4293; (c) K. Mashima, K. H. Kusano, Y. I. Matsumura, K. Nozaki, H. Kumobayashi, N. Sayo, Y. Hori and T. Ishizaki, *J. Org. Chem.*, 1994, **59**, 3064.
- R. Noyori, Nobel Lecture: Asymmetric Catalysis: Science and Opportunities, <https://www.nobelprize.org/prizes/chemistry/2001/noyori/lecture/>, accessed January 17, 2021.
- (a) H. Pellissier, *Coord. Chem. Rev.*, 2017, **336**, 96; (b) A. L. Reznichenko and K. C. Hultsch, *Organometallics*, 2013, **32**, 1394; (c) J. Y. Kim and T. Livinghouse, *Org. Lett.*, 2005, **7**, 1737.
- (a) N. N. Greenwood and A. Earnshaw, *Chemistry of the Elements*, 2nd edn, Butterworth-Heinemann, Oxford, 1997, pp. 1230–1242; (b) Wiley-VCH, *Ullmann's Encyclopedia of Industrial Chemistry*, Wiley-VCH, Weinheim, 2005; (c) G. Haxel, J. Hedrick and J. Orris, *Rare earth elements critical resources for high technology*, United States Geological Survey, Reston, 2006.
- (a) S. Harder, in *Early Maingroup Metals in Catalysis: Concepts and Reactions*, Wiley-VCH, Weinheim, Germany, 2019; (b) S. Harder, *Chem. Rev.*, 2010, **110**, 3852; (c) S. Harder, F. Feil and K. Knoll, *Angew. Chem., Int. Ed.*, 2001, **40**, 4261; (d) M. H. Chisholm, J. Gallucci and K. Phomphrai, *Chem. Commun.*, 2003, 48; (e) F. Buch, J. Brettar and S. Harder, *Angew. Chem., Int. Ed.*, 2006, **118**, 2807; (f) M. R. Crimmin, A. G. M. Barrett, M. S. Hill, P. B. Hitchcock and P. A. Procopiu, *Organometallics*, 2008, **27**, 497; (g) S. Ziemann, S. Kriek, H. Görls and M. Westerhausen, *Organometallics*, 2018, **37**, 924; (h) H. Bauer, M. Alonso, C. Fischer, B. Rösch, H. Elsen and S. Harder, *Angew. Chem., Int. Ed.*, 2018, **57**, 15177; (i) M. He, M. T. Gamer and P. W. Roesky, *Organometallics*, 2016, **35**, 2638.
- M. S. Hill, D. J. Liptrot and C. Weetman, *Chem. Soc. Rev.*, 2016, **45**, 972.
- (a) Y. Yamashita, T. Tsubogo and S. Kobayashi, *Early Maingroup Metals in Catalysis: Concepts and Reactions*, ed. S. Harder, Wiley-VCH, Weinheim, Germany, 2019, pp. 311–345; (b) T. Poisson, Y. Yamashita and S. Kobayashi, *J. Am. Chem. Soc.*, 2010, **132**, 7890; (c) S. Kobayashi and Y. Yamashita, *Acc. Chem. Res.*, 2011, **44**, 58; (d) T. Tsubogo, Y. Yamashita and S. Kobayashi, *Angew. Chem., Int. Ed.*, 2009, **48**, 9117.
- S. Neal, A. Ellern and A. Sadow, *J. Organomet. Chem.*, 2011, **696**, 228.
- P. Horrillo-Martinez and K. Hultsch, *Tetrahedron Lett.*, 2009, **50**, 2054.
- X. Zhang, T. Emge and K. Hultsch, *Angew. Chem., Int. Ed.*, 2012, **51**, 394.
- B. Schmid, S. Frieß, A. Herrera, A. Linden, F. Heinemann, H. Locke, S. Harder and R. Dorta, *Dalton Trans.*, 2016, **45**, 12028.
- F. Buch and S. Harder, *Z. Naturforsch., B: J. Chem. Sci.*, 2008, **63**, 169.
- J. Wixey and B. Ward, *Dalton Trans.*, 2011, **40**, 7693.
- J. Wixey and B. Ward, *Chem. Commun.*, 2011, **47**, 5449.
- D. Nixon and B. Ward, *Chem. Commun.*, 2012, **48**, 11790.
- P. C. Stegner, C. A. Fischer, D. T. Nguyen, A. Rösch, J. Penafiel, J. Langer, M. Wiesinger and S. Harder, *Eur. J. Inorg. Chem.*, 2020, **35**, 3387.
- J. Penafiel, *Alkaline earth organometallic compounds in homogeneous catalysis*, PhD thesis, University of Groningen, 2016.
- S. Bestgen and P. W. Roesky, *Early Maingroup Metals in Catalysis: Concepts and Reactions*, ed. S. Harder, Wiley-VCH, Weinheim, Germany, 2019, pp. 59–91.
- (a) C. Glock, H. Görls and M. Westerhausen, *Chem. Commun.*, 2012, **48**, 7094; (b) F. M. Younis, S. Kriek, H. Görls and M. Westerhausen, *Organometallics*, 2015, **34**, 3577; (c) F. M. Younis, S. Kriek, H. Görls and M. Westerhausen, *Dalton Trans.*, 2016, **45**, 6241; (d) S. Kriek, D. Kalden, A. Oberheide, L. Seyfarth, H. D. Arndt, H. Görls and M. Westerhausen, *Dalton Trans.*, 2019, **48**, 2479.

- 21 (a) V. Vasilenko, C. K. Blasius, H. Wadepohl and L. H. Gade, *Chem. Commun.*, 2020, **56**, 1203; (b) A. Falconnet, M. Magre, B. Maity, L. Cavallo and M. Rueping, *Angew. Chem.*, 2019, **131**, 17731.
- 22 (a) T. X. Gentner, B. Rösch, K. Thum, J. Langer, G. Ballmann, J. Pahl, W. A. Donaubauer, F. Hampel and S. Harder, *Organometallics*, 2019, **38**, 2485; (b) B. Freitag, J. Pahl, C. Färber and S. Harder, *Organometallics*, 2018, **37**, 469; (c) C. N. de Bruin-Dickason, T. Sutcliffe, C. A. Lamsfus, G. B. Deacon, L. Maron and C. Jones, *Chem. Commun.*, 2018, **54**, 786; (d) A. Arrowsmith, B. Maitland, G. Kociok-Köhn, A. Stasch, M. S. Hill and C. Jones, *Inorg. Chem.*, 2014, **53**, 10543; (e) M. Rauch, S. Ruccolo and G. Parkin, *J. Am. Chem. Soc.*, 2017, **139**, 13264.
- 23 (a) B. Freitag, P. Stegner, K. Thum, C. A. Fischer and S. Harder, *Eur. J. Inorg. Chem.*, 2018, **18**, 1938; (b) B. Freitag, C. A. Fischer, J. Penafiel, G. Ballmann, H. Elsen, C. Färber, D. F. Piesik and S. Harder, *Dalton Trans.*, 2017, **46**, 11192.
- 24 G. R. Clemo and E. C. Dawson, *J. Chem. Soc.*, 1939, 1114.
- 25 S. Quideau, G. Lyvinec, M. Marguerit, K. Bathany, A. Ozanne-Beaudenon, T. Buffeteau, D. Cavagnat and A. Chenede, *Angew. Chem., Int. Ed.*, 2009, **48**, 4605.
- 26 N. Miyano and H. Mori, *Bull. Chem. Soc. Jpn.*, 1984, **57**, 2171.
- 27 K. Huynh, T. Livinghouse and H. N. Lovick, *Synlett*, 2014, **25**, 1721.
- 28 C. Zang, Y. Liu, Z.-J. Xu, C.-W. Tse, X. Guan, J. Wei, J. S. Huang and C. M. Che, *Angew. Chem., Int. Ed.*, 2016, **55**, 10253.
- 29 C. C. Scarborough, B. V. Popp, I. A. Guzei, G. A. Ilia and S. S. Stahl, *J. Organomet. Chem.*, 2005, **690**, 6143.
- 30 R. R. Fraser, T. S. Mansour and S. Savard, *J. Org. Chem.*, 1985, **50**, 3232.
- 31 M. Rodriguez, I. Zubiri, H. L. Milton, D. J. Cole-Hamilton, A. M. Z. Slawin and J. D. Woollins, *Polyhedron*, 2004, **23**, 693.
- 32 R. D. Shannon, *Acta Crystallogr.*, 1976, **32**, 751.
- 33 M. D. Jones, F. A. A. Paz, J. E. Davies and B. F. G. Johnson, *Acta Crystallogr., Sect. E: Struct. Rep. Online*, 2003, **59**, 910.
- 34 M. E. Jung and G. Piizzi, *Chem. Rev.*, 2005, **105**, 1735.
- 35 M. R. Crimmin, M. Arrowsmith, A. G. M. Barrett, I. J. Casely, M. S. Hill and P. A. Procopiou, *J. Am. Chem. Soc.*, 2009, **131**, 9670.
- 36 X. Zhang, S. Tobisch and K. C. Hultsch, *Chem. – Eur. J.*, 2015, **21**, 7841.